MRS **C**ommunications

Functional Oxides Prospective Article

A perspective on perovskite oxide semiconductor catalysts for gas phase photoreduction of carbon dioxide

Chunxiang Huang, Zhaosheng Li, and **Zhigang Zou,** National Laboratory of Solid State Microstructures, College of Engineering and Applied Sciences, Ecomaterials and Renewable Energy Research Center (ERERC), Nanjing University, No. 22 Hankou Road, Nanjing 210093, People's Republic of China

Address all correspondence to Zhaosheng Li or Zhigang Zou at **zsli@nju.edu.cn** or **zgzou@nju.edu.cn**

Abstract

Photocatalytic reduction of carbon dioxide (CO_2) into renewable hydrocarbon fuels using solar energy has gained much attention in the effort to conserve energy and enhance carbon cycling. This paper begins with a brief description of the basic concepts of the photocatalytic reduction of CO_2, introduces some experimental challenges in the gas photoreaction system and provides a review of perovskite oxide semiconductor catalysts, including tantalates, niobates, titanates, zirconates and cerates, for use in the gas phase photoreduction of CO_2. The prospects for the future research of CO_2 photoreduction are also presented.

Introduction

Recently, there are increasing concerns of energy and environmentalism due, in part, to the growing consumption of non-renewable fossil fuels and the rising atmospheric levels of carbon dioxide (CO_2), a major greenhouse gas that is considered to be a major contributor to global warming and other unforeseen severe consequences. The photocatalytic reduction of CO_2 into hydrocarbons using solar energy, often referred to as artificial photosynthesis, is believed to be a potential and promising approach to solve both issues.[1–5] Since the reduction of CO_2 by a TiO_2 photocatalyst was reported by Inoue and Fujishima's group,[6] the photocatalytic reduction of CO_2 has attracted the attention of many researchers. The key to this process is to develop an efficient photocatalyst that can properly position the valence and conduction bands for the oxidation and reduction half-reactions of water and CO_2, respectively.[5,7] To date, various photocatalysts (such as TiO_2,[8] CdS,[9] GaP,[10] Zn_2GeO_4,[11] etc.) have been used for photocatalytic CO_2 reduction. Usually, the photocatalysts with an ideal perovskite structure are expected to exhibit good photocatalytic activity, which has been demonstrated in many studies.[12,13] Recently, a series of perovskite type materials of the form ABO_3 (such as $BaZrO_3$,[14] $BaCeO_3$,[15] $SrTiO_3$,[16] etc.) have been studied in the photocatalytic reduction of CO_2.

Although the photocatalytic reduction of CO_2 has been well studied, the conversion efficiency of CO_2 is still very low compared with that of water splitting.[3,4] Two major photocatalytic systems are being studied: a solid–liquid interface prepared by an aqueous dispersion of photocatalysts and a solid–gas interface.[5] Usually, both the liquid-phase (CH_3OH, HCHO, HCOOH) and gas-phase (CH_4) products can be detected in a liquid photoreaction system, whereas only gas-phase (CH_4, CO) products could be detected in a gas photoreaction system.[7] Although the solid–liquid reaction interface increases the accessible area for carriers and reactants, this approach has two drawbacks: the rather low solubility of CO_2 and the reduction of water competing with CO_2 reduction in the aqueous suspensions. Although the solid–gas reaction interface promotes the separation of products and reactants, the ratio of gaseous CO_2 and H_2O is easily tunable, which thus inhibits competitive water reduction.[17,18] Because the products of the photocatalytic reduction of CO_2 are mostly C1 compounds, it is necessary to eliminate the effects of any organic or carbon residues on the whole photocatalytic reaction process because organic molecules (e.g., acetic acid) or carbon residues may undergo the photo-Kolbe reaction, photodegradation, photolysis reactions or reverse disproportionation reactions on the photocatalyst.[19,20]

This paper begins with a brief description of the basic concepts of the photocatalytic reduction of CO_2 and introduces some experimental problems encountered in the gas photoreaction system. In addition, this paper reviews perovskite oxide semiconductor catalysts used in the photocatalytic reduction of CO_2. The prospects for future developments of CO_2 photoreduction are also presented.

Basic concepts of the photocatalytic reduction of CO_2

CO_2 photoreduction is the conversion of CO_2 into hydrocarbon fuels using sunlight, which is also known as artificial photosynthesis. Because CO_2 is one of the most thermodynamically stable carbon compounds and because it cannot absorb light in the
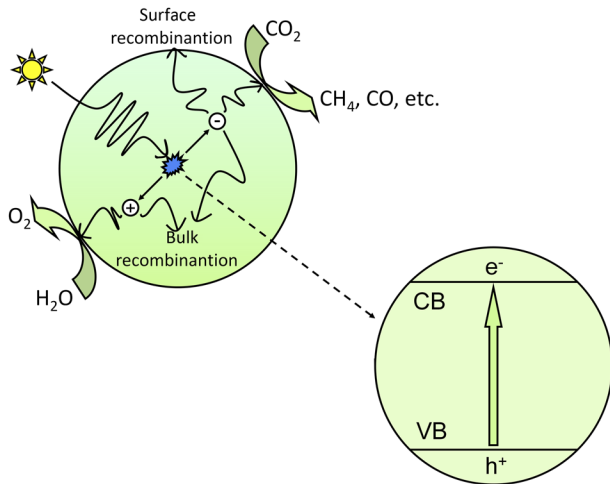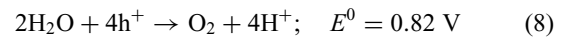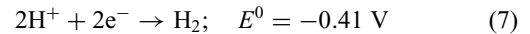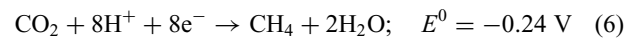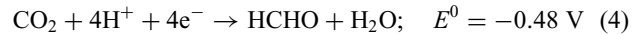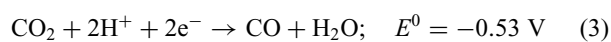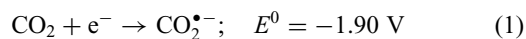
Figure 1. Schematic illustration of the photoexcitation and electron transfer process for the photocatalytic reduction of CO_2 with H_2O as a reductant.

wavelengths of 200–900 nm, the CO_2 photoreduction process requires a suitable photosensitizer, which is generally a semiconductor catalyst.[21,22] Figure 1 shows the basic mechanism for the photocatalytic process of CO_2 reduction. In the photocatalytic process, photons having energy greater than or equal to the band gap energy are absorbed by the semiconductor, and the electrons in the valence band (VB) are excited to the conduction band (CB). Consequently, equal numbers of electrons and holes are generated in the CB and VB, respectively. The photogenerated electron–hole pairs separate from each other and transfer to the active sites on the surface of semiconductors; then, the photogenerated electrons with strong reduction potential reduce CO_2 into hydrocarbons such as CH_4 and CO, etc., and the photogenerated holes with strong oxidation potential oxidize H_2O into O_2.

However, not all photogenerated electron–hole pairs reaching the surface of semiconductor catalysts can participate in the redox reaction, as the energy of the photogenerated electron–hole pairs must meet a certain thermodynamic conditions.[5,21] That is, the bottom of the CB of the semiconductor photocatalysts should have a more negative potential than the reduction potential of CO_2 forming HCOOH, CO, HCHO, CH_3OH and CH_4; likewise, the top of the VB should have a more positive potential than the oxidation potential of H_2O. Equations (1)–(8) show the possible reactions involved in CO_2 photoreduction and their corresponding theoretical potentials (vs. the normal hydrogen electrode in an aqueous solution at pH 7 and 25°C, assuming unit activity).[4,5,21]

$$CO_2 + e^- \rightarrow CO_2^{\bullet-}; \quad E^0 = -1.90 \text{ V} \quad (1)$$

$$CO_2 + 2H^+ + 2e^- \rightarrow HCOOH; \quad E^0 = -0.61 \text{ V} \quad (2)$$

$$CO_2 + 2H^+ + 2e^- \rightarrow CO + H_2O; \quad E^0 = -0.53 \text{ V} \quad (3)$$

$$CO_2 + 4H^+ + 4e^- \rightarrow HCHO + H_2O; \quad E^0 = -0.48 \text{ V} \quad (4)$$

$$CO_2 + 6H^+ + 6e^- \rightarrow CH_3OH + H_2O; \quad E^0 = 0.38 \text{ V} \quad (5)$$

$$CO_2 + 8H^+ + 8e^- \rightarrow CH_4 + 2H_2O; \quad E^0 = -0.24 \text{ V} \quad (6)$$

$$2H^+ + 2e^- \rightarrow H_2; \quad E^0 = -0.41 \text{ V} \quad (7)$$

$$2H_2O + 4h^+ \rightarrow O_2 + 4H^+; \quad E^0 = 0.82 \text{ V} \quad (8)$$

From a thermodynamic point of view,[21,23] the reaction of one electron to form $CO_2^{\bullet-}$ is highly unfavorable due to the very negative reduction potential of -1.9 V (vs. NHE) for this process [Eq. (1)]. Thus, many researchers believe that the photocatalytic reduction of CO_2 is a multi-electronic process, which requires less energy for electron transfer compared with a mono-electronic process [Eqs. (2)–(6)]. In the multi-electron CO_2 reduction pathway, the reaction requires the assistance of a corresponding number of protons [Eq. (8)]. The formation of products could be different, which is determined by the number of photogenerated electron–hole pairs participating in the redox reaction.

Although photocatalytic reduction of CO_2 has been well studied, the CO_2 conversion efficiency of this process is still very low. In addition to a suitable E_g and CB potential, many factors influence the conversion efficiency of the multi-electron CO_2 photocatalytic reduction process. These factors include excitation, transport, separation (recombination) of the photogenerated electron–hole pairs, the adsorption capacity of the gas molecules, the reduction of CO_2, the oxidation of H_2O, and so on. Furthermore, the selective formation of specific products is also a considerable problem in the photocatalytic reduction of CO_2.[3,4] So far, many strategies, including increased visible-light excitation (e.g., impurity doping, sensitization,[24] and solid solution construction[25]), improved transport and separation of the photogenerated electron–hole pairs (e.g., loading with cocatalysts,[26] synthesis of nanostructured photocatalysts,[27] and construction of semiconductor heterojunctions[28]), enhanced adsorption of CO_2 (e.g., increasing the surface area[29]), and suppression off-target side reactions (e.g., the competitive reaction of H_2O reduction in Eq. (7)[30]), etc., have been designed to achieve a high efficiency and selectivity.
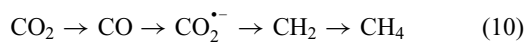
Key points of the experimental details

The efficiency of the photocatalytic reduction of CO_2 depends not only on the factors mentioned above, a suitable semiconductor photocatalyst (with proper E_g, CB and VB), the excitation, transport and separation (recombination) of the photogenerated electron–hole pairs, etc., but also on the experimental conditions,[20,31–33] such as the light source, response time, reaction temperature, the ratio of H_2O and CO_2, etc.

Photocatalytic reduction of CO_2 is mainly carried out at room pressure and temperature and is controlled by a cooling water recirculation system. A high pressure mercury lamp

and/or a 300 W xenon lamp, usually with a cutoff filter, are the most common light sources in CO_2 photoreduction. Yahaya et al. found that the traditional UV lamp had a drawback in that the light intensity would decrease with rising temperature due to the lengthy illumination time, and this decrease affects the efficiency of CO_2 photocatalytic reduction.[31] The selection of response time for the studies of CO_2 photoreduction is different, ranging from tens of minutes to hours. Zhao et al. studied nano-sized CoPc/TiO_2 particles as a catalyst for photoconversion of CO_2 and discussed the effect of irradiation time on the formation of photo-reduced products over a period of 6–50 h.[32] At short reaction times, the product yields increased rapidly because more photoelectrons were generated with increasing time of light exposure; however, the product yields flattened out after 20 h of irradiation. This result can be attributed to saturation of the reactive surface active sites absorbed with intermediate products. In addition, the molar ratio of H_2O and CO_2 is also found to play an important role in determining the reaction rate and product selectivity for CO_2 photocatalytic reduction. Zhang et al. investigated the photocatalytic reduction of CO_2 with H_2O on a Pt-loaded TiO_2 catalyst and studied the effect of the H_2O/CO_2 molar ratio on CH_4 yield. They found that the CH_4 yield of 0.15 wt.% Pt-loaded TiO_2 nanotube increased as the mole ratio of H_2O and CO_2 increased, while the different H_2O:CO_2 molar ratios had little effect on the CH_4 yield of 0.12 wt.% Pt-loaded TiO_2 nanoparticles.[33] The formation of CH_4 occurred mainly due to the high concentration of the surface OH group, which had been shown previously by Ikeue et al.[34]

The main products in a gas phase reaction system for photocatalytic reduction of CO_2 are generally CH_4, which is usually on the μmol scale, as well as a small amount of CO.[8,14–16] As we mentioned above, the photocatalytic reduction of CO_2 is a complex multi-electronic reaction process. There are two plausible pathways for CH_4 formation[4,20]:
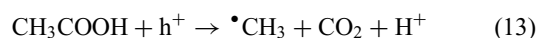
$$CO_2 \rightarrow HCOOH \rightarrow HCHO \rightarrow CH_3OH \rightarrow CH_4 \quad (9)$$

$$CO_2 \rightarrow CO \rightarrow CO_2^{\bullet-} \rightarrow CH_2 \rightarrow CH_4 \quad (10)$$

It is necessary to verify whether the carbon source for CH_4 production is actually the CO_2 for the gaseous CO_2 reduction because any organic adsorbates or carbon residues may take part in side reactions, such as the photo-Kolbe reaction, mineralization reaction, photolysis reaction or reverse disproportionation reaction.[19,20] These reactions could create a false impression of the formation of hydrocarbon products.

If there are any carbon residues deposited or buried on the surface of catalyst during the preparation of the catalyst for the photocatalytic reduction of CO_2, a reverse disproportionation reaction of the impurity might occur in the presence of CO_2 in the reaction system. In this case, the generated CO would react with the water adsorbed on the surface active sites of the catalyst; then, the generated CH_3OH would ultimately generate CH_4. This pathway has been shown by Yang

et al. through the combined use of in situ diffuse reflectance infrared Fourier transform spectroscopy (DRIFTS) and ^{13}C labeled CO_2 during CO_2 photoreduction over Cu-promoted crystalline TiO_2 catalysts. The reaction process could be described as follows[19,35]:

$$C \text{ (impurity in or on catalyst)} + CO_2 \rightarrow CO + CO \quad (11)$$

$$CO + 2H_2O \rightarrow CH_3OH + O_2 \quad (12)$$
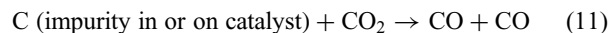
Yui et al. demonstrated that organic adsorbates, especially CH_3COOH, had a significant effect on the formation of CH_4 in CO_2 photoreduction over TiO_2. The organic adsorbed on the surface of TiO_2 could participate in a so-called photo-Kolbe reaction (CH_3COOH, for example)[36]:

$$CH_3COOH + h^+ \rightarrow {}^\bullet CH_3 + CO_2 + H^+ \quad (13)$$

$${}^\bullet CH_3 + CH_3COOH \rightarrow {}^\bullet CH_2COOH + CH_4 \quad (14)$$

In addition, if there are any alcohols and O_2 in the CO_2 photoreduction reaction system producing CH_4, CO_2 would be generated in-situ due to the mineralization of alcohols on the surface of the semiconductor photocatalyst, which could be explained through the following mechanism[20]:

$$\text{Organic radical (OR)} + O_2 \rightarrow CO_2 \quad (15)$$
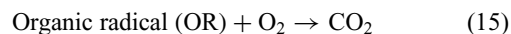
In conclusion, evaluations of the products for CO_2 photocatalytic reduction should be interpreted with caution. In other words, the C source should be carefully investigated with respect to the production of CH_4 and CO from CO_2 in a gaseous CO_2 photoreduction system. Most researchers carry out a series of contrast experiments with different conditions including H_2O, CO_2, irradiation and catalyst to exclude the effects of carbon residues and organic adsorbates on the formation of hydrocarbon products[14–16]; some other studies, however, reported a more precise and intuitive method: isotopic labeling (^{13}C and ^{18}O).[35–37] This approach can simultaneously evaluate the C source and the O source. To guarantee the reliability of the results of CO_2 photocatalytic reduction, carbon residues or organic adsorbates must be avoided throughout the entire reaction system. These residues and adsorbates may form during the synthesis of the catalyst if it involves the use of alkoxides and organic solvents (e.g., polyethylene glycol, PEG) as precursors or in washing steps if organic cleaning solvents are used.[35,38,39] These residues could be removed using particular methods, such as thermal treatment in a continuous flow of N_2 or Ar inert gas or at high temperature in air, as well as prolonged washing in a water environment.[19,35,36]

Perovskite oxide semiconductor photocatalysts for gaseous CO_2 reduction

An ideal semiconductor photocatalyst for CO_2 photoreduction should benefit from: (1) a suitable E_g such that the

semiconductor absorbs incident photons over a range of wavelengths to generate electron–hole pairs; (2) effective separation between the photogenerated electron–hole pairs that then transfer to the surface of semiconductors and subsequently take part in the oxidation-reduction reaction with CO_2 and H_2O absorbed on the surface active sites of the semiconductors; and (3) a well-tuned CB and VB such that the bottom of the CB is located at a more negative potential than the reduction potentials of CO_2 and such that the top of the VB has a more positive potential than the oxidation potential of H_2O. Based on these principles, various photocatalysts, including metal oxides (e.g., TiO_2,[8] ZnO,[40] $BiVO_4$,[41] and Ga_2O_3[42]), metal sulfides (e.g., CdS[9] and ZnS[43]), metal phosphides (e.g., GaP[10]), nitrides (e.g., C_3N_4[44]), etc., have been reported for CO_2 reduction. Among them, perovskite oxide semiconductor photocatalysts are good candidates for CO_2 reduction due to their unique physical and chemical properties, including their stability, their controllable structure and their ability to be doped in two different cation sites. In addition, perovskite structures are expected to exhibit good photocatalytic activity as has been demonstrated in many studies.[12,13] Recently, a series of the perovskite type materials of the form ABO_3 (such as $BaZrO_3$,[14] $BaCeO_3$,[15] $SrTiO_3$,[16,45,46] etc.) have been studied for the photocatalytic reduction of CO_2. Table I shows the summary of perovskite oxide semiconductors used in the photocatalytic reduction of CO_2 in a gas reaction system. These semiconductors were roughly divided into five types: tantalates, niobates, titanates, zirconates and cerates.

Tantalates

Teramura et al. carried out the photoreduction of CO_2 over $ATaO_3$ (A = Li, Na and K) synthesized by a conventional solid-state reaction in the presence of H_2. CO was the only gaseous product over all of the samples tested under 200 W Hg-Xe lamp irradiation.[54] $LiTaO_3$ presented the highest activity for CO yield (0.42 μmol/g in 24 h), and the trend of the photocatalytic activities were consistent with that of the E_g ($LiTaO_3 > NaTaO_3 > KTaO_3$). In addition, they also found that the amount of evolved CO gas depended on the amount of chemisorbed CO_2 (as shown in Fig. 2),[54] which meant that the adsorption of CO_2 had an effect on the reduction efficiency of CO_2. H_2 was used as reductant in this photocatalytic reduction of CO_2 process, whereas other gas reaction systems usually used H_2O as reductant.

Niobates

Niobates with a perovskite structure share many characteristics with tantalates and have been used in CO_2 photocatalytic reduction systems with water as the reductant. Shi et al. studied the photocatalytic reduction activities of CO_2 into CH_4 over $NaNbO_3$ samples upon irradiation from a Xe arc lamp. It was discovered that the CH_4 evolution rate (653 ppm/h/g) of Pt-loaded $NaNbO_3$ nanowires prepared by a hydrothermal method were much higher than that of bulk $NaNbO_3$ particles synthesized by a solid-state reaction.[53] Subsequently, they

prepared alkali niobate $ANbO_3$ (A = K, Na) photocatalysts using a conventional solid-state reaction method and compared their photocatalytic performance for CO_2 reduction under similar conditions. They found that $KNbO_3$ (7.0 ppm/h) showed a higher photocatalytic activity than $NaNbO_3$ (2.3 ppm/h).[52] The perovskite $NaNbO_3$ studied in most research has a typical cubic structure, whereas $NaNbO_3$ also has another crystal structure—an orthorhombic structure. The schematic crystal structures of cubic and orthorhombic $NaNbO_3$ are shown in Fig. 3.[51] Li et al. discussed the photocatalytic activities of CO_2 reduction over the cubic and orthorhombic $NaNbO_3$ in a gas phase system and found that the CO_2 reduction activity over the cubic $NaNbO_3$ was nearly twice that of the orthorhombic $NaNbO_3$. These results might be due to the unique electron structure of cubic $NaNbO_3$, which may support electron excitation and transfer.[51] In addition, they studied the influence of the preparation temperature on the activity of $NaNbO_3$ photocatalyst.[50] The cubic $NaNbO_3$ prepared at 500°C presented the best photocatalytic performances, and the CH_4 evolution for gas phase CO_2 photoreduction over $NaNbO_3$ loaded with 0.5 wt.% Pt under a 300 W Xe lamp ($\lambda > 300$ nm) could reach 12.6 μmol/m^2/h.

Moreover, differing from the simple ABO_3-type perovskite semiconduction photocatalysts, lamellar perovskite niobates, such as HNb_3O_8 and KNb_3O_8, have also been applied in the gas phase photocatalytic reduction of CO_2.[48,49] Figure 4 shows a schematic drawing of the layered structures of HNb_3O_8 composed of 2D $Nb_3O_8^-$ anion thin sheets of edge- and corner-shared NbO_6 octahedral with H^+ intercalated between the layers. Li et al. found that hydrothermally synthesized HNb_3O_8 and KNb_3O_8 nanobelts exhibited much higher yields of CH_4 compared with the HNb_3O_8 and KNb_3O_8 particles prepared by conventional solid-state reactions as well as commercial TiO_2.[48]

Titanates

Several perovskite titanates, such as $SrTiO_3$, $PbTiO_3$ and $CaTiO_3$, have also been explored for gas phase CO_2 photocatalytic reduction.[16,45–47] Among them, $SrTiO_3$ is the most widely studied photocatalysts. Xie et al. prepared a self-doped $SrTiO_{3-\delta}$ using a carbon-free one-step combustion, and they demonstrated that the chemical adsorption of CO_2 could be improved by increasing the oxygen deficiency of the $SrTiO_3$. This deficiency promoted the photocatalytic activity of CO_2 reduction to generate CH_4 under visible light irradiation.[16] Zhou et al. discussed a leaf-shaped 3D hierarchical artificial photosynthetic system of $ATiO_3$ (A = Sr, Ca and Pb) prepared by a modified sol-gel method using fresh green leaves as a structure template. They studied the effects of various cocatalysts (Au, Ag, Cu, Pt, RuO_2 and NiO_x) on the photocatalytic activity of CO_2. As shown in Fig. 5, CH_4 and CO were the two main products, and Au as a suitable cocatalyst exhibited the best performance for the selectivity of both CH_4 and CO (using $SrTiO_3$ as an example).[45] In another study, Kou et al. synthesized a highly active photocatalyst with response to visible light by

Table I. Summary of perovskite oxide semiconductors for the photocatalytic reduction of CO_2 in a gas reaction system.

Catalyst/band gap energy	Co-catalyst	Reaction medium	Light source	Major products	Yield[a]	References
$BaZrO_3$/4.8 eV	0.3 wt.% Ag	CO_2 and H_2O vapor	300 W Xe lamp (PE 300BUV)	CH_4	0.57	14
$BaCeO_3$/3.2 eV	0.3 wt.% Ag	CO_2 and H_2O vapor	300 W Xe lamp (PE 300BUV)	CH_4	0.55	15
$SrTiO_{3-\delta}$/3.2 eV	Self-doped 0.3 wt.% Pt	CO_2 and H_2O vapor	300 W Xe lamp $\lambda > 420$ nm	CH_4	0.25[b]	16
$SrTiO_3$/3.2 eV	1 wt.% Au	CO_2 and H_2O vapor	300 W Xe lamp $\lambda > 420$ nm	CH_4 CO	CH_4: 0.231 CO: 0.349	45
$CaTiO_3$/3.5 eV	1 wt.% Au	CO_2 and H_2O vapor	300 W Xe lamp $\lambda > 420$ nm	CH_4 CO	CH_4: 0.029	45
$PbTiO_3$/2.9 eV	1 wt.% Au	CO_2 and H_2O vapor	300 W Xe lamp $\lambda > 420$ nm	CH_4 CO	CH_4: 0.007	45
$SrTiO_3$/3.2 eV	0.02Co doped Pt loaded	CO_2 Gas-closed system	300 W Xe lamp $\lambda > 420$ nm	CH_4	63.6[c]	46
$Ca_xTi_yO_3$/3.44 eV ($x = y = 1$)	–	CO_2 and H_2O vapor	6 W/cm^2 UV lamp $\lambda = 365$ nm	CH_4	17[d]	47
HNb_3O_8/3.66 eV nanobelts	–	CO_2 and H_2O vapor	350 W Xe lamp	CH_4	3.58	48
HNb_3O_8/3.5 eV SiO_2-HNb_3O_8/3.5 eV	0.4 wt.% Pt	CO_2 and H_2O vapor	350 W Xe lamp	CH_4	0.47 2.90	49
KNb_3O_8/3.66 eV nanobelts	–	CO_2 and H_2O vapor	350 W Xe lamp	CH_4	1.71	48
$NaNbO_3$/3.25 eV	0.5 wt.% Pt	CO_2 Gas-closed system	350 W Xe lamp $\lambda > 300$ nm	CH_4	12.6[b]	50
c-$NaNbO_3$/3.29 eV o-$NaNbO_3$/3.45 eV	0.5 wt.% Pt	CO_2 and H_2O vapor	300 W Xe lamp	CH_4	0.486 0.245	51
$NaNbO_3$/3.4 eV	0.5 wt.% Pt	CO_2 and H_2O vapor	300 W Xe lamp	CH_4	2.3[c]	52
$KNbO_3$/3.1 eV	0.5 wt.% Pt	CO_2 and H_2O vapor	300 W Xe lamp	CH_4	7.0[c]	52
$NaNbO_3$/3.4 eV nanowires	0.5 wt.% Pt	CO_2 and H_2O vapor	300 W Xe lamp	CH_4	653[e]	53
$LiTaO_3$/4.9 eV	–	CO_2 and H_2	200 W Hg-Xe lamp	CO	0.42[f]	54
$NaTaO_3$/4.1 eV	–	CO_2 and H_2	200 W Hg-Xe lamp	CO	0.1[f]	54
$KTaO_3$/3.7 eV	–	CO_2 and H_2	200 W Hg-Xe lamp	CO	0.06[f]	54

[a]Maximum formation rate reported for the products in μmol/h/g, unless stated otherwise.

[b]In μmol/m$^2_{cata}$/h.

[c]In ppm/h.

[d]The entire yield for the main products in μmol/g (7 h, $x = y = 1$).

[e]In ppm/h/g.

[f]The entire yield for the main products in μmol/g (24 h).

substituting the Ti^{4+} in $SrTiO_3$ to transition metal (Co, Fe, Ni) ions for gas phase CO_2 reduction, and Pt-$SrTi_{0.98}Co_{0.02}O_3$ had the highest activity (the yield of CH_4 was 63.6 ppm/h).[46]

Zirconates

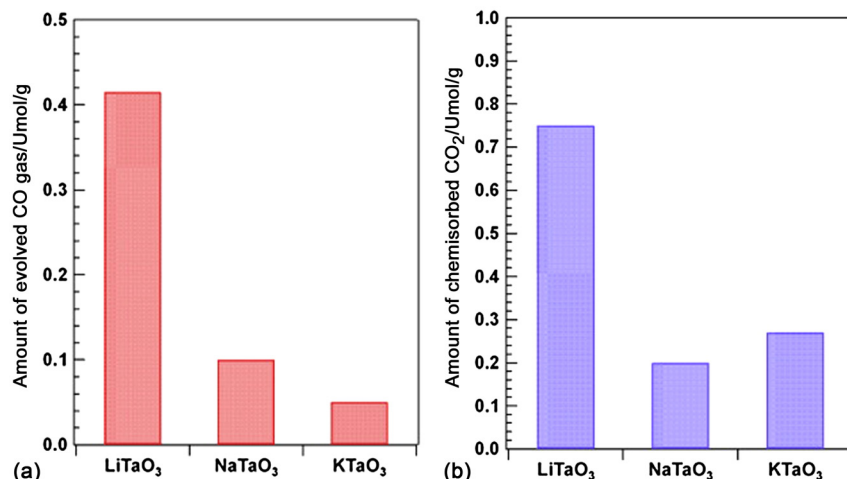Apart from the above-mentioned tantalates, niobates and titanates photocatalysts, Chen et al. first investigated the

Figure 2. (a) Amount of evolved CO gas for the photocatalytic reduction of CO_2 in the presence of H_2 as a reductant over $ATaO_3$ (A = Li, Na, K) after 24 h of photoirradiation. (b) Amount of Chemisorbed CO_2 on $ATaO_3$ (A = Li, Na, K). (Copyright 2010, Applied Catalysis B: Environmental.[54]).

photocatalytic properties of $BaZrO_3$ for CO_2 reduction into CH_4 in a gas reaction system.[14] Barium zirconate made by the Pechini process has a bandgap of 4.8 eV, which means that $BaZrO_3$ only has a UV light response. They also confirmed the effects of different cocatalysts on the photocatalytic activities and optimized the loaded amount of metal nanoparticle co-catalysts. As shown in Fig. 6, Ag was a suitable cocatalyst that

exhibited the best selectivity for producing CH_4 with the $BaZrO_3$ system. In addition, a CH_4 yield of up to 0.57 μmol/h/g was obtained when 0.3 wt.% Ag cocatalyst was loaded onto the surface of the $BaZrO_3$. In this case, the Ag site acted as an electron trap to effectively decrease the recombination rate of the photogenerated electron–hole pairs.

Cerates

All the perovskite oxide semiconductor photocatalysts for CO_2 reduction mentioned above consist of metal cations with d^0 (Zr^{4+}, Ti^{4+}, Nb^{5+}, or Ta^{5+}) configurations. Wang et al. first reported the photocatalytic properties of $BaCeO_3$, whose conduction band mainly consists of Ce 4f orbitals, as a new photocatalyst for gas phase CO_2 reduction.[15] The activity of
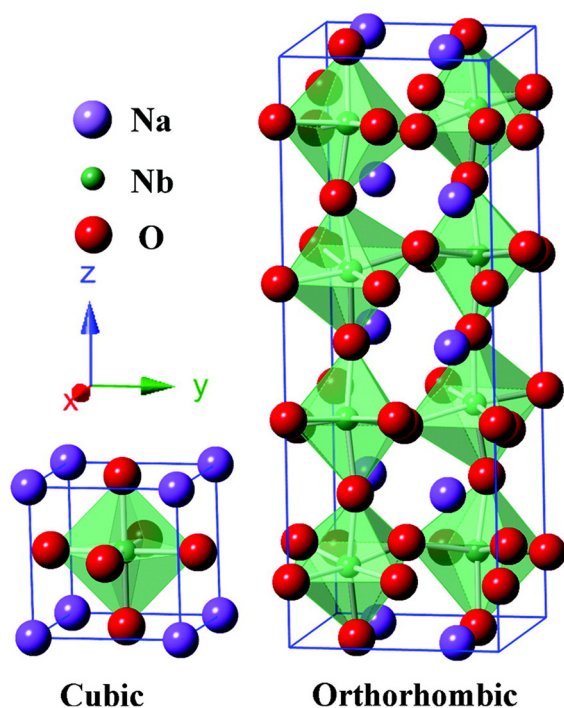

Figure 3. Schematic crystal structures of cubic and orthorhombic $NaNbO_3$. (Copyright 2012, The Journal of Physical Chemistry.[51]).
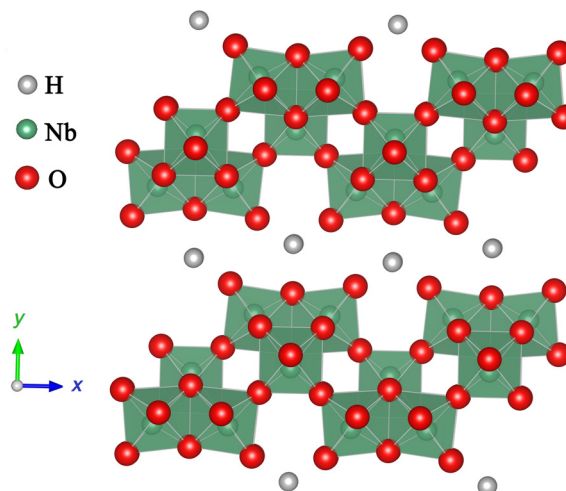

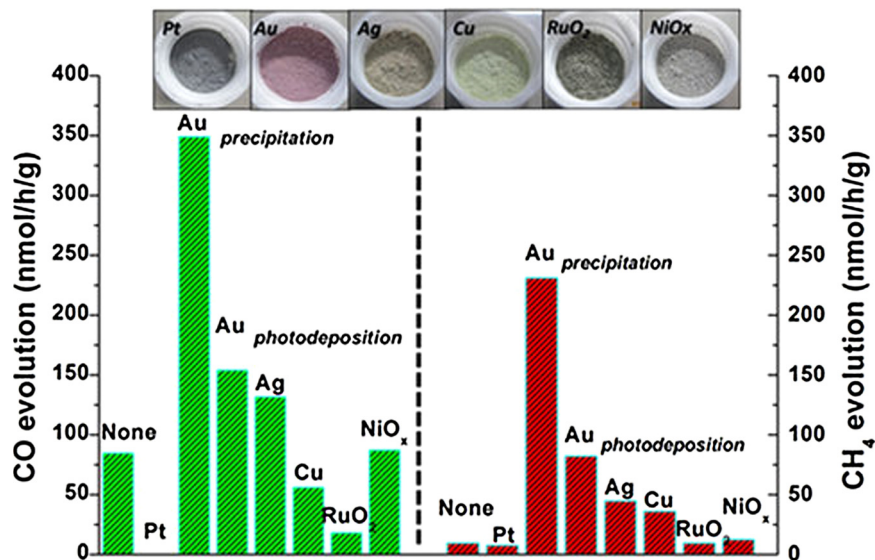**Figure 4.** Schematic drawing of the layered structures of HNb_3O_8.

Figure 5. CO and CH_4 evolution on an artificial photosynthetic system of $SrTiO_3$ of CO_2 photoreduction loaded with different cocatalysts. (Copyright 2013, Scientific Reports.[45]).

photocatalytic reduction of CO_2 into CH_4 over $BaCeO_3$ loaded with 0.3 wt% Ag cocatalyst was up to 0.55 µmol/h/g. This experiment proved that perovskite-type oxide semiconductor photocatalysts with conduction bands dominated by 4f electronic configuration could also react as well as the semiconductor photocatalysts with d^0 electronic configuration in gas phase CO_2 photoreduction.

Summary and outlook

The photocatalytic reduction of CO_2 into renewable hydrocarbon fuels using solar energy is a promising approach for simultaneously achieving carbon cycling and solving the shortage of sustainable energy. An ideal semiconductor photocatalyst for

CO_2 photoreduction should have a suitable E_g and proper positioning of the CB and VB, which should satisfy thermodynamic conditions of CO_2 reduction. In addition, the photogenerated electron–hole pairs should separate effectively and transfer to the surface active sites of the semiconductor photocatalysts so that they can participate in the oxidation-reduction reactions with CO_2 and H_2O.

The photocatalytic reduction of CO_2 is a complex multi-electronic reaction process. The main products in a gas phase CO_2 reduction are generally CH_4 as well as a small amount of CO, and the yield of CH_4 is usually on the µmol scale. This yield is relatively low compared with the conversion of water splitting.[14–16,45–54] The conversion efficiency and
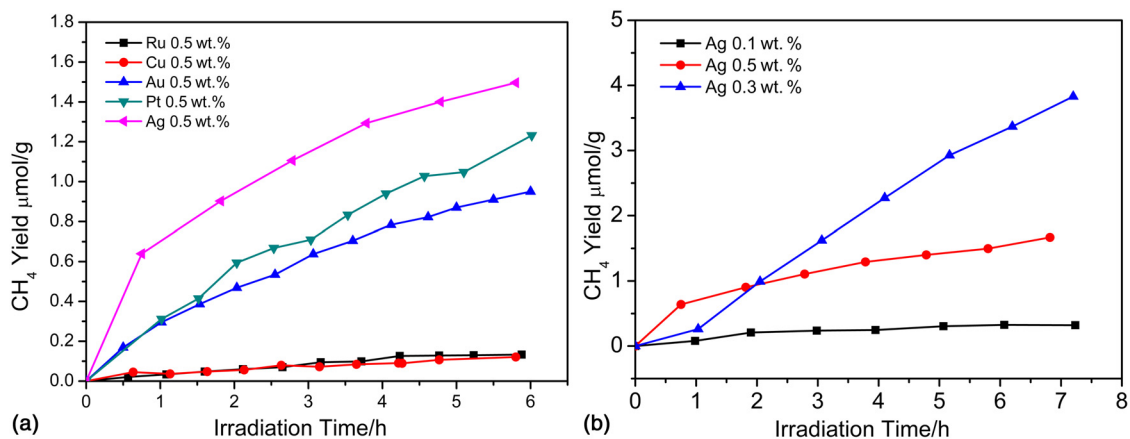

Figure 6. (a) CH_4 yields of $BaZrO_3$ deposited with different cocatalysts (Ru, Cu, Au, Pt, Ag) of the same apparent amount. (b) CH_4 yields of $BaZrO_3$ with different amounts of Ag deposition. (Copyright 2015, Catalysis Science & Techonology.[14]).

products selectivity of gaseous CO_2 photoreduction not only depends on the characteristics of the photocatalyts but also depends on some experimental conditions, such as the light source, response time, reaction temperature, the ratio of H_2O and CO_2, etc. It is necessary to verify whether the formation of hydrocarbon products is actually from the photocatalytic reduction of CO_2 or is from some side reactions with organic adsorbates (e.g., acetic acid) or carbon residues. These adsorbates or residues may be formed during the photo-Kolbe reaction, mineralization reaction or reverse disproportionation reaction in photocatalytic reaction. A series of contrast experiments with different conditions (including H_2O, CO_2, irradiation and catalyst) or a more intuitive and precise method—isotopic labeling (^{13}C and ^{18}O)—is necessary to detect and/or exclude the effects of carbon residues and organic adsorbates. These contaminants can also be removed by thermal treatment in air or inert gas or by prolonged washing with water upon the formation of products.

Based on the research and the current development of related theories and practical applications, the photocatalytic reduction of CO_2 still has a long way to go. The future studies on CO_2 photoreduction should be initiated in the following areas.

Developing a new suitable photocatalyst

As we mentioned above, a wide variety of perovskite oxide semiconductors system have been applied to the photocatalytic reduction of CO_2 in a gas reaction system under UV or visible light irradiation. Most of them consist of metal cations with d^0 configurations including tantalates, niobates, titanates, zirconates, with the exception being cerates such as $BaCeO_3$ with 4f orbitals electron configurations. It is believed that perovskite oxide semiconductor photocatalysts still have great prospects due to their unique physical and chemical properties in the future study of the photocatalytic reduction of CO_2. For example, alkaline earth stannates of $MSnO_3$ (M = Ca, Sr and Ba), which contain Sn^{4+} ions with a d^{10} electronic configuration, have been used as the photocatalyst applied to photocatalytic reactions for H_2 and O_2 evolution in water splitting.[55] The bottom of the CBs are located at -1.46, -1.37 and -0.69 V (versus NHE, pH = 7) for $CaSnO_3$, $SrSnO_3$ and $BaSnO_3$, respectively, while the top of the VBs are 2.98, 2.69 and 2.41 V (versus NHE, pH = 7), respectively. Thus, the photogenerated electrons in the CB are more negative than the reduction potentials of CO_2 into HCOOH, CO, HCHO, CH_3OH and CH_4, and the corresponding photogenerated holes in the VB can easily oxidize H_2O in the ABO_3 structure of these stannates. In other words, $MSnO_3$ (M = Ca, Sr and Ba) is theoretically feasible as a photocatalyst for the reduction of CO_2. In addition, our group has already tested the photocatalytic reduction of CO_2 over $BaSnO_3$, and we hope that $MSnO_3$ (M = Ca, Sr and Ba) will be a promising photocatalyst for the gas phase photoreduction of CO_2 in future.

In addition, double perovskite oxides with the general chemical formula of $A_2BB'O_6$ have attracted much interest due to their variable crystal structures, flexible chemical compositions and other unique physicochemical properties such as being semi-metallic. These catalysts have been successfully applied to water splitting, such as Ba_2InTaO_6 with a E_g of ca. 4.17 eV.[56] A variety of elements are available for substitution into the A or B site; B site elements are usually transition metals with d-orbital configurations, and A site elements are usually alkaline earth ions such as Ca, Sr and Ba.[57] Based on these results, development of new double perovskite oxide semiconductors system seem to be one feasible direction for research on CO_2 reduction in future.

Cocatalysts

It is generally believed that cocatalysts play a crucial role in semiconductor-based photocatalysis.[3,4,58] Firstly, loaded cocatalysts could serve as electron traps to promote the separation of photogenerated electron–hole pairs resulting from the formation of a Schottky barrier between the semiconductor and the cocatalyst. Hence, they could improve the photocatalytic activity and selectivity for CO_2 reduction. Secondly, cocatalysts could effectively lower the activation barrier of CO_2 due to their better conductivity and lower over potential.[59,60] To date, a series of cocatalysts including Pd, Pt, Au, Ag, Ru, Cu, Ni, Co, etc. have been used for photocatalytic reactions, and each presented different effects on the conversion efficiency.[26,45,61] In addition, it is worth noticing that the bimetallic cocatalyst systems (such as Cu and Pt) have also exhibited good activities for CO_2 reduction,[62] and the enhancement mechanism is still unclear. Thus, it is essential to better understand the photocatalytic mechanism of cocatalysts and to develop cheap, abundant and highly efficient cocatalyst systems (e.g., non-noble metal cocatalysts and new-type bifunctional cocatalysts with a proper structure) for the photocatalytic reduction of CO_2.

Gas adsorption ability on the surface of photocatalysts

It is well known that the reduction of CO_2 and the oxidation of H_2O are the two main half-reaction steps for the photocatalytic reduction of CO_2. On one hand, effective adsorption of CO_2 is an important process that can be promoted by increasing surface area,[29] by introducing basic sites such as MgO, or by introducing surface oxygen vacancies[16,63]. Optimization of adsorption is important for improving the conversion efficiency for the photocatalytic reduction of CO_2. The adsorption of CO_2 molecules on stoichiometric and oxygen-deficient $SrTiO_3$ has been theoretically and experimentally studied by Xie et al. They demonstrated that chemical adsorption of CO_2 molecules could be improved by increasing the oxygen deficiency in $SrTiO_3$, thus enhancing the photocatalytic performance for CO_2 reduction.[16] On the other hand, water oxidation favors the efficient separation of the photogenerated electron–hole pairs, thus improving the photocatalytic activity for CO_2 reduction.[3,19] In addition, deactivation of the photocatalysts may occur after long reaction times, which may be attributed to the active sites gradually becoming covered by the adsorption

of the reduction intermediate products or the final products accumulation on the photocatalyst surface over time.[32,64] In conclusion, it is important to refine the research on the adsorption of gaseous reactants (CO_2, H_2O) and the products on the surface of photocatalysts.

In short, the future development for the photocatalytic reduction of CO_2 remains challenging, and the comprehensive efforts (such as materials synthesis, doping, nanostructuring and heterojunction)[4,25] are needed to achieve a breakthrough in the conversion efficiency of CO_2 reduction into hydrocarbon fuels that may eventually lead to industrialization.

Acknowledgments

References

1. Z.S. Li, J.Y. Feng, S.C. Yan, and Z.G. Zou: Solar fuel production: strategies and new opportunities with nanostructures. *Nano Today* **10**, 468 (2015).
2. J.L. White, M.F. Baruch, J.E. Pander III, Y. Hu, I.C. Fortmeyer, J.E. Park, T. Zhang, K. Liao, J. Gu, Y. Yan, T.W. Shaw, E. Abelev, and A.B. Bocarsly: Light-driven heterogeneous reduction of carbon dioxide: photocatalysts and photoelectrodes. *Chem. Rev.* **115**, 12888 (2015).
3. X. Li, J.Q. Wen, J.X. Low, Y.P. Fang, and J.G. Yu: Design and fabrication of semiconductor photocatalyst for photocatalytic reduction of CO_2 to solar fuel. *Sci. China Mater.* **57**, 70 (2014).
4. W.G. Tu, Y. Zhou, and Z.G. Zou: Photocatalytic conversion of CO_2 into renewable hydrocarbon fuels: state-of-the-art accomplishment, challenges, and prospects. *Adv. Mater.* **26**, 4607 (2014).
5. K.F. Li, X.Q. An, K.H. Park, M. Khraisheh, and J.W. Tang: A critical review of CO_2 photoconversion: catalysts and reactors. *Catal. Today* **224**, 3 (2014).
6. T. Inoue, A. Fujishima, S. Konishi, and K. Honda: Photoelectrocatalytic reduction of carbon dioxide in aqueous suspensions of semiconductor powders. *Nature* **277**, 637 (1979).
7. S.N. Habisreutinger, L. Schmidt-Mende, and J.K. Stolarczyk: Photocatalytic reduction of CO_2 on TiO_2 and other semiconductors. *Angew. Chem. Int. Ed.* **52**, 7372 (2013).
8. L.J. Liu, H.L. Zhao, J.M. Andino, and Y. Li: Photocatalytic CO_2 reduction with H_2O on TiO_2 nanocrystals: comparison of anatase, rutile, and brookite polymorphs and exploration of surface chemistry. *ACS Catal.* **2**, 1817 (2012).
9. S. Wang and X. Wang: Photocatalytic CO_2 reduction by CdS promoted with a zeolitic imidazolate framework. *Appl. Catal. B-Environ.* **162**, 494 (2015).
10. E.E. Barton, D.M. Rampulla, and A.B. Bocarsly: Selective solar-driven reduction of CO_2 to methanol using a catalyzed p-GaP based photoelectrochemical cell. *J. Am. Chem. Soc.* **130**, 6342 (2008).
11. S.C. Yan, J.J. Wang, and Z.G. Zou: An anion-controlled crystal growth route to Zn_2GeO_4 nanorods for efficient photocatalytic conversion of CO_2 into CH_4. *Dalton Trans.* **42**, 12975 (2013).
12. H. Kato and A. Kudo: Water splitting into H_2 and O_2 on alkali tantalite photocatalysts $ATaO_3$(A=Li, Na, and K). *J. Phys. Chem. B* **105**, 4285 (2001).
13. A. Kudo, H. Kato, and S. Nakagawa: Water splitting into H_2 and O_2 on new $Sr_2M_2O_7$ (M=Nb and Ta) photocatalysts with layered perovskite structure: factors affecting the photocatalytic activity. *J. Phys. Chem. B.* **104**, 571 (2000).
14. X.L. Chen, J. Wang, C.X. Huang, S.Y. Zhang, H.T. Zhang, Z.S. Li, and Z.G. Zou: Barium zirconate: a new photocatalyst for converting CO_2 into hydrocarbons under UV irradiation. *Catal. Sci. Technol.* **5**, 1758 (2015).
15. J. Wang, C.X. Huang, X.L. Chen, H.T. Zhang, Z.S. Li, and Z.G. Zou: Photocatalytic CO_2 reduction of $BaCeO_3$ with 4f configuration electrons. *Appl. Surf. Sci.* **358**, 463 (2015).
16. K. Xie, N. Umezawa, N. Zhang, P. Reunchan, Y.J. Zhang, and J.H. Ye: Self-doped $SrTiO_{3-\delta}$ photocatalyst with enhanced activity for artificial photosynthesis under visible light. *Energy Environ. Sci.* **4**, 4211 (2011).
17. K. Mori, H. Yamashita, and M. Anpo: Photocatalytic reduction of CO_2 with H_2O on various titanium oxide photocatalysts. *RSC Adv.* **2**, 3165 (2012).
18. M. Anpo and K. Chiba: Photocatalytic reduction of CO2 on anchored titanium oxide catalysts. *J. Mole. Catal.* **74**, 207 (1992).
19. Y. Izumi: Recent advances in the photocatalytic conversion of carbon dioxide to fuels with water and/or hydrogen using solar energy and beyond. *Coordin. Chem. Rev.* **257**, 171 (2013).
20. G.R. Dey: Chemical reduction of CO_2 to different products during photo catalytic reaction on TiO_2 under diverse conditions: an overview. *J. Nat. Gas Chem.* **16**, 217 (2007).
21. V.P. Indrakanti, J.D. Kubicki, and H.H. Schobert: Photoinduced activation of CO_2 on Ti-based heterogeneous catalysts: current state, chemical physics-based insights and outlook. *Energy Environ. Sci.* **2**, 745 (2009).
22. S.C. Roy, O.K. Varghese, M. Paulose, and C.A. Grimes: Toward solar fuels: photocatalytic conversion of carbon dioxide to hydrocarbons. *ACS Nano* **4**, 1259 (2010).
23. J. Schneider, H. Jia, J.T. Muckerman, and E. Fujita: Thermodynamics and kinetics of CO_2, CO, and H^+ binding to the metal centre of CO_2 reduction catalysts. *Chem. Soc. Rev.* **41**, 2036 (2012).
24. S. Sato, T. Morikawa, S. Saeki, T. Kajino, and T. Motohiro: Visible-light-induced selective CO_2 reduction utilizing a ruthenium complex electrocatalyst linked to a p-type nitrogen-doped Ta_2O_5 Semiconductor. *Angew. Chem. Int. Ed.* **49**, 5101 (2010).
25. N. Zhang, S.X. Ouyang, T. Kako, and J.H. Ye: Mesoporous zinc germanium oxynitride for CO_2 photoreduction under visible light. *Chem. Commun.* **48**, 1269 (2012).
26. O. Ishitani, C. Inoue, Y. Suzuki, and T. Ibusuki: Photocatalytic reduction of carbon dioxide to methane and acetic acid by an aqueous suspension of metal-deposited TiO_2. *J. Photochem. Photobio. A: Chem.* **72**, 269 (1993).
27. B.J. Liu, T. Torimoto, H. Matsumoto, and H. Yoneyama: Effect of solvents on photocatalytic reduction of carbon dioxide using TiO_2 nanocrystal photocatalyst embedded in SiO_2 matrices. *J. Photochem. Photobio. A: Chem.* **108**, 187 (1997).
28. G.C. Xi, S.X. Ouyang, and J.H. Ye: General synthesis of hybrid TiO_2 mesoporous "french fries" toward improved photocatalytic conversion of CO_2 into hydrocarbon fuel: a case of TiO_2/ZnO. *Chem. Eur. J.* **17**, 9057 (2011).
29. D.K. Wang, R.K. Huang, W.J. Liu, D.R. Sun, and Z.H. Li: Fe-based MOFs for photocatalytic CO_2 reduction: role of coordination unsaturated sites and dual excitation pathways. *ACS Catal.* **4**, 4254 (2014).
30. Q.G. Zhai, S.J. Xie, W.Q. Fan, Q.H. Zhang, Y. Wang, W.P. Deng, and Y. Wang: Photocatalytic conversion of carbon dioxide with water into methane: platinum and copper(I) oxide co-catalysts with a core-shell structure. *Angew. Chem.* **125**, 5888 (2013).
31. A.H. Yahaya, M.A. Gondal, and A. Hameed: Selective laser enhanced photocatalytic conversion of CO_2 into methanol. *Chem. Phys. Lett.* **400**, 206 (2004).
32. Z.H. Zhao, J.M. Fan, S.H. Liu, and Z.Z. Wang: Optimal design and preparation of titania-supported CoPc using sol-gel for the photo-reduction of CO_2. *Chem. Eng. J.* **151**, 134 (2009).
33. Q.H. Zhang, W.D. Han, Y.J. Hong, and J.G. Yu: Photocatalytic reduction of CO_2 with H_2O on Pt-loaded TiO_2 catalyst. *Catal. Today* **148**, 335 (2009).
34. K. Ikeue, S. Nozaki, M. Ogawa, and M. Anpo: Characterization of self-standing Ti-containing porous silica thin films and their reactivity for the photocatalytic reduction of CO_2 with H_2O. *Catal. Today* **74**, 241 (2002).
35. C.C. Yang, Y.H. Yu, B. van der Linden, and J.C.S. Wu: Artificial photosynthesis over crystalline TiO_2-based catalysts: fact or fiction? *J. Am. Chem. Soc.* **132**, 8398 (2010).
36. T. Yui, A. Kan, C. Saitoh, K. Koike, T. Ibusuki, and O. Ishitani: Photochemical reduction of CO_2 using TiO_2: effects of organic adsorbates

on TiO_2 and deposition of Pd onto TiO_2. *ACS Appl. Mater. Inter.* **3**, 2594 (2011).

37. P. Li, Y. Zhou, H.J. Li, Q.F. Xu, X.G. Meng, X.Y. Wang, M. Xiao, and Z.G. Zou: All-solid-state Z-scheme system arrays of $Fe_2V_4O_{13}$/RGO/CdS for visible light-driving photocatalytic CO_2 reduction into renewable hydrocarbon fuel. *Chem. Commun.* **51**, 800 (2015).

38. K. Kočí, L. Obalová, L. Matějová, D. Plácháa, Z. Lacnýa, J. Jirkovskýc, and O. Šolcová: Effect of TiO_2 particle size on the photocatalytic reduction of CO_2. *Appl. Catal. B: Environ.* **89**, 494 (2009).

39. W.Y. Lin and H. Frei: Bimetallic redox sites for photochemical CO_2 splitting in mesoporous silicate sieve. *Comptes Rendus Chimie.* **9**, 207 (2006).

40. G. Mahmodi, S. Sharifnia, F. Rahimpour, and S.N. Hosseini.: Photocatalytic conversion of CO_2 and CH_4 using ZnO coated mesh: effect of operational parameters and optimization. *Solar Energy Mater. Solar Cells* **111**, 31 (2013).

41. Y.Y. Liu, B.B. Huang, Y. Dai, X.Y. Zhang, X.Y. Qin, M.H. Jiang, and M.H. Whangbo: Selective ethanol formation from photocatalytic reduction of carbon dioxide in water with $BiVO_4$ photocatalyst. *Catal. Commun.* **11**, 210 (2009).

42. H. Park, J.H. Choi, K.M. Choi, D.K. Lee, and J.K. Kang: Highly porous gallium oxide with a high CO_2 affinity for the photocatalytic conversion of carbon dioxide into methane. *J. Mater. Chem.* **22**, 5304 (2012).

43. H. Fujiwara, H. Hosokawa, K. Murakoshi, Y. Wada, and S. Yanagida: Surface characteristics of ZnS nanocrystallites relating to their photocatalysis for CO_2 reduction1. *Langmuir* **14**, 5154 (1998).

44. J. Mao, T.Y. Peng, X.H. Zhang, K. Li, L.Q. Ye, and L. Zan: Effect of graphitic carbon nitride microstructures on the activity and selectivity of photocatalytic CO_2 reduction under visible light. *Catal. Sci. Technol.* **3**, 1253 (2013).

45. H. Zhou, J.J. Guo, P. Li, T.X. Fan, D. Zhang, and J.H. Ye: Leaf-architectured 3D hierarchical artificial photosynthetic system of perovskite titanates towards CO_2 photoreduction into hydrocarbon fuels. *Sci. Rep.* **3**, 1 (2013).

46. J.H. Kou, J. Gao, Z.S. Li, H. Yu, Y. Zhou, and Z.G. Zou: Construction of visible-light-responsive $SrTiO_3$ with enhanced CO_2 adsorption ability: highly efficient photocatalysts for artifical photosynthesis. *Catal. Lett.* **145**, 640 (2015).

47. B.S. Kwak and M. Kang: Photocatalytic reduction of CO_2 with H_2O using perovskite $Ca_xTi_yO_3$. *Appl. Surf. Sci.* **337**, 138 (2015).

48. X.K. Li, H.Q. Pan, W. Li, and Z.J. Zhuang: Photocatalytic reduction of CO_2 to methane over HNb_3O_8 nanobelts. *Appl. Catal. A: Gen.* **413–414**, 103 (2012).

49. X.K. Li, W. Li, Z.J. Zhuang, Y.S. Zhong, Q. Li, and L.Y. Wang: Photocatalytic reduction of carbon dioxide to methane over SiO_2-pillared HN_3O_8. *J. Phys. Chem. C.* **116**, 16047 (2012).

50. P. Li, S.X. Ouyang, Y.J. Zhang, T. Kako, and J.H. Ye: Surface-coordination-induced selective synthesis of cubic and orthorhombic $NaNbO_3$ and their photocatalytic properties. *J. Mater. Chem. A.* **1**, 1185 (2013).

51. P. Li, S.X. Ouyang, G.C. Xi, T. Kako, and J.H. Ye: The effects of crystal structure and electronic structure on photocatalytic H_2 evolution and CO_2 reduction over two phases of perovskite-structured $NaNbO_3$. *J. Phys. Chem. C.* **116**, 7621 (2012).

52. H.F. Shi and Z.G. Zou: Photophysical and photocatalytic properties of $ANbO_3$ (A=Na, K) photocatalysts. *J. Phys. Chem. Solids* **73**, 788 (2012).

53. H.F. Shi, T.Z. Wang, J. Chen, C. Zhu, J.H. Ye, and Z.G. Zou: Photoreduction of carbon dioxide over $NaNbO_3$ nanostructured photocatalysts. *Catal. Lett.* **141**, 525 (2011).

54. K. Teramura, S. Okuoka, H. Tsuneoka, T. Shishido, and T. Tanaka: Photocatalytic reduction of CO_2 using H_2 as reductant over $ATaO_3$ photocatalysts (A=Li, Na, K). *Appl. Catal. B: Environ.* **96**, 565 (2010).

55. W.F. Zhang, J.W. Tang, and J.H. Ye: Structural, photocatalytic, and photophysical properties of perovskite $MSnO_3$ (M=Ca, Sr, and Ba) photocatalysts. *J. Mater. Res.* **22**, 1859 (2007).

56. K. Song, J. Yang, P.F. Jiang, W.L. Gao, R.H. Cong, and T. Yang: Ba_2InTaO_6-A partially B-site-ordered double perovskite for overall water splitting. *Eur. J. Inorg. Chem.* **2015**, 5786 (2015).

57. L. Li, Q. Gao, G. Lei, H.H. Xie, J.B. Deng, and X.R. Hu: First-principles investigations on electronic and thermodynamic properties of double perovskite Sr_2XMoO_6 (X=Ge and Si). *J. Phys. Chem. Solids* **94**, 30 (2016).

58. J.H. Yang, D.G. Wang, H.X. Han, and C. Li: Roles of cocatalysts in photocatalysis and photoelectrocatalysis. *Acc. Chem. Res.* **46**, 1900 (2013).

59. F.E. Osterloh and B.A. Parkinson: Recent developments in solar water-splitting photocatalysis. *MRS Bull.* **36**, 17 (2011).

60. K. Maeda and K. Domen: Photocatalytic water splitting: recent progress and future challenges. *J. Phys. Chem. Lett.* **1**, 2655 (2010).

61. S. Fukuzumi, D. Hong, and Y. Yamada: Bioinspired photocatalytic water reduction and oxidation with earth-abundant metal catalysts. *J. Phys. Chem. Lett.* **4**, 3458 (2013).

62. O.K. Varghese, M. Paulose, T.J. LaTempa, and C.A. Grimes: High-rate solar photocatalytic conversion of CO_2 and water vapor to hydrocarbon fuels. *Nano Lett.* **9**, 731 (2009).

63. S.J. Xie, Y. Wang, Q.H. Zhang, W.P. Deng, and Y. Wang: MgO- and Pt-promoted TiO_2 as an efficient photocatalyst for the preferential reduction of carbon dioxide in the presence of water. *ACS Catal.* **4**, 3644 (2014).

64. Z. Xiong, Y.C. Zhao, J.Y. Zhang, and C.G. Zheng: Efficient photocatalytic reduction of CO_2 into liquid products over cerium doped titania nanoparticles synthesized by a sol-gel auto-ignited method. *Fuel Process. Technol.* **135**, 6 (2015).